Improving the Thermal and Mechanical Properties of Poly(propylene carbonate) by Incorporating Functionalized Graphite Oxide

J. Bian,[1] X. W. Wei,[1] S. J. Gong,[1] H. Zhang,[1] Z. P. Guan[2]

[1]*Key Laboratory of Special Materials and Preparation Technologies, School of Materials Science & Engineering, Xi-hua University, Chengdu, Sichuan 610039, People's Republic of China*
[2]*Department of Chemistry, National University of Singapore, Singapore 117543, Republic of Singapore*

Received 25 February 2011; accepted 12 May 2011
DOI 10.1002/app.34897
Published online 31 August 2011 in Wiley Online Library (wileyonlinelibrary.com).

ABSTRACT: Poly(propylene carbonate) (PPC) is a new biodegradable aliphatic polycarbonate. However, the poor thermal stability, low glass transition temperatures (T_g), and relatively low mechanical property have limited its applications. To improve the thermal and mechanical properties of PPC, functionalized graphite oxide (MGO) was synthesized and mixed with PPC by a solution intercalation method to produce MGO/PPC composites. A uniform structure of MGO/PPC composites was confirmed by X-ray diffraction and scanning electron microscope. The thermal and mechanical properties of MGO/PPC composites were investigated by thermal gravimetric analysis, differential scanning calorimetric, dynamic mechanical analysis, and electronic tensile tester. Due to the nanometer-sized dispersion of layered graphite in polymer matrix, MGO/PPC composites exhibit improved thermal and mechanical properties than pure PPC. When the MGO content is 3.0 wt %, the MGO/PPC composites shows the best thermal and mechanical properties. These results indicate that nanocomposition is an efficient and convenient method to improve the properties of PPC. © 2011 Wiley Periodicals, Inc. J Appl Polym Sci 123: 2743–2752, 2012

Key words: poly(propylene carbonate) (PPC); graphite oxide (GO); composites; structure and morphology; thermal and mechanical properties

INTRODUCTION

Biodegradable polymers are of increasing interest and attracting much attention from the material researchers and industry, because of the increasing environmental concerns about waste pollution.[1,2] Poly(propylene carbonate) (PPC) is a new biodegradable aliphatic polycarbonate and it has a potentially wide range of applications, such as binder resins and packing materials. In addition, the ester bonds in the macromolecular backbone chains supply the molecular chain flexibility and good melt flow characteristics. However, the poor thermal stability and relatively low mechanical property of PPC has limited its applications.[3]

Recently, great efforts have been devoted to improve the deficient thermal and mechanical property of PPC, including the chemical method such as "grafting"[4] and the physical method such as "filling."[5–7] Among these methods, the filling is commercially advantageous because the physical properties are readily manipulated by the type and concentration of fillers.[8] However, for conventional filler/PPC composites, the high loading level of fillers leads to the deterioration of some properties. Therefore, it is still a challenging work to obtain PPC composites with superior properties with a quite low filler addition.

Natural graphite is composed of layered nanosheets.[9] Recently, polymer/graphite nanosheet composites have been intensively studied because of their excellent properties.[10–13] The weak interplanar forces allow for certain atoms, molecules, and ions to intercalate into the interplanar spaces of the graphite.[9] However, unlike the layered clay, there are no reactive ionic groups on the surface of the original layered graphite.[11] Thus, it is very difficult to prepare polymer intercalated or exfoliated polymer composite. Xu et al. prepared intercalated-exfoliated organophilic montmorillonite (OMMT)/PPC composites by direct melt blending.[14] It was reported that some undesired problems such as thermal degradation of PPC and loss of mechanical property could occur during the melt compounding.[15] Du et al. prepared MgAl/PPC layered double hydroxide (MgAl-LDH/PPC) exfoliated composites by solution intercalation.[16] It was pointed out that the organic modified MgAl-LDH

Correspondence to: J. Bian (bianjun2003@163.com) Z. P. Guan (nusguanzhp@hotmail.com).
Contract grant sponsor: Key Research Fund Program of Xihua University; contract grant number: Z0910109.

additive could catalyze the degradation of PPC resin. Zhang et al. prepared maleated PPC composites (OMMT/PPC-MA) by using commercial OMMT as filler, owing to the reaction between hydroxyl groups (OH) of OMMT and carboxyl groups (COOH) PPC-MA chains, the OMMT can disperse more fully in matrix.[17] However, it is still a challenging work to obtain the complete exfoliated structure of layered fillers in the polymer matrix although many methods have been developed.[18–21]

Graphite oxide (GO) has been proposed as a novel substitute of graphite for the fabrication of polymer/graphite composite.[15,22–24] Upon oxidation, some functional groups can be introduced in the structure of graphite.[25] The presence of these functional groups makes graphene oxide sheets strongly hydrophilic, which allows GO to readily swell and disperse in water[26] and alkaline solutions.[27] Unfortunately, owing to their hydrophilic nature, graphene oxide sheets can only be dispersed in aqueous media that are incompatible with most organic polymers. To enhance the dispersibility of GO in aprotic polar solvents and compatibility with polymer matrix, Stankovich et al.[28,29] have demonstrated that the exfoliation behavior of GO could be altered by changing the surface properties of graphene oxide sheets by way of chemical functionalization (e.g., by treating GO with organic isocyanates). As a result, such isocyanate-derivatized GO no longer exfoliate in water but readily form stable dispersions in polar aprotic solvents, such as *N*, *N*-dimethylformamide (DMF). The dispersion of isocyanate-derivatized GO allows graphene oxide sheets to be intimately mixed with many organic polymers, facilitating the synthesis of graphene–polymer composites. Xu et al.[30] have treated the surface of GO with tolylene-2,4-diisocyanate (TDI) to create the anchor sites on GO and couple with amphiphilic oligoester through a "grafting to" approach to improve the dispersibility of modified GO in both water and organic media. The "grafting to" approach is to graft available polymers which normally possess terminal functional groups on the surface of the substrate.[31]

In this article, we report a facile method for preparation of MGO/PPC composites with excellent thermal stability and mechanical property. GO was firstly treated with TDI to create the anchor sites on GO. Then, GO-TDI was reacted with 1,4-butanediol (BD) through the "grafting to" method to afford hydroxyl groups on the surface of GO. The BD-derived hydroxyl groups on the surface of GO will be effective as "grafting points" of PPC. Further, the hydrogen bond interaction between TDI and PPC chains can be strengthened. The structure of functionalized GO (MGO) and MGO/PPC composites was elucidated by using Fourier transform infrared spectroscopy (FTIR), X-ray diffraction (XRD), atomic force microscope (AFM), and scanning electron microscopy (SEM). The influences of MGO on the thermal and mechanical properties of MGO/PPC composites were investigated.

EXPERIMENTAL

Materials

PPC sample with a number-average molecular weight (M_n) of 27,000 was kindly provided by Tian-Guan Group (Hei-Nan, China). The natural graphite powder (NGP, SP-2, ($C > 99\%$, $D = 5$ μm)) were purchased from Qingdao Tianhe Graphite Co., Ltd. (Qing-Dao, China). Potassium permanganate (C.P), sulfuric acid (>96%), hydrogen peroxide, BD, acetone, anhydrous DMF, TDI, and dehydrated toluene were purchased from Ke-Long Reagent, Inc. (Chen-Du, China) and used as received.

Preparation process of GO, GO-TDI, and MGO (GO-TDI-BD)

GO used in this research was synthesized according to the procedures depicted in Ref. [32]. The synthetic procedure of MGO (GO-TDI-BD) was shown in Scheme 1. GO-TDI-BD was prepared by modifying the method originally proposed by Xu et al.[30] The obtained GO was modified by an excess amount of TDI. Subsequently, an excessive BD was added into this suspension. In this synthesis procedure, GO (2 g) was loaded into a 100-mL three-necked flask equipped with a magnetic stirring bar, and 100 mL DMF dehydrated was then added under nitrogen to create an in-homogenous suspension. The TDI (2 g) was next added and the mixture was stirred under nitrogen at 80°C for 24 h. After 24 h, the excessive BD (5 g) was added into the slurry reaction mixture under nitrogen atmosphere and then reacted for 24 h at 80°C. The suspension was poured into acetone (50 mL) to coagulate the product, followed by centrifugation and washing several times to remove the un-reacted BD. Finally, the resulting product (marked as GO-TDI-BD) was dried at 100°C under vacuum for 48 h before use.

Preparation of MGO/PPC composites

The MGO/PPC composites were prepared by solution intercalation. First, a solution of a certain amount of MGO dispersed in 25 mL DMF was sonicated for 30 min, and mechanically stirred for another 10 min. After then, the PPC was added to the above-mentioned solution and continuously stirred for 24 h at 40°C for polymer intercalation. The mixed solution was poured into a Petri-dish, and dried in a vacuum at room temperature to

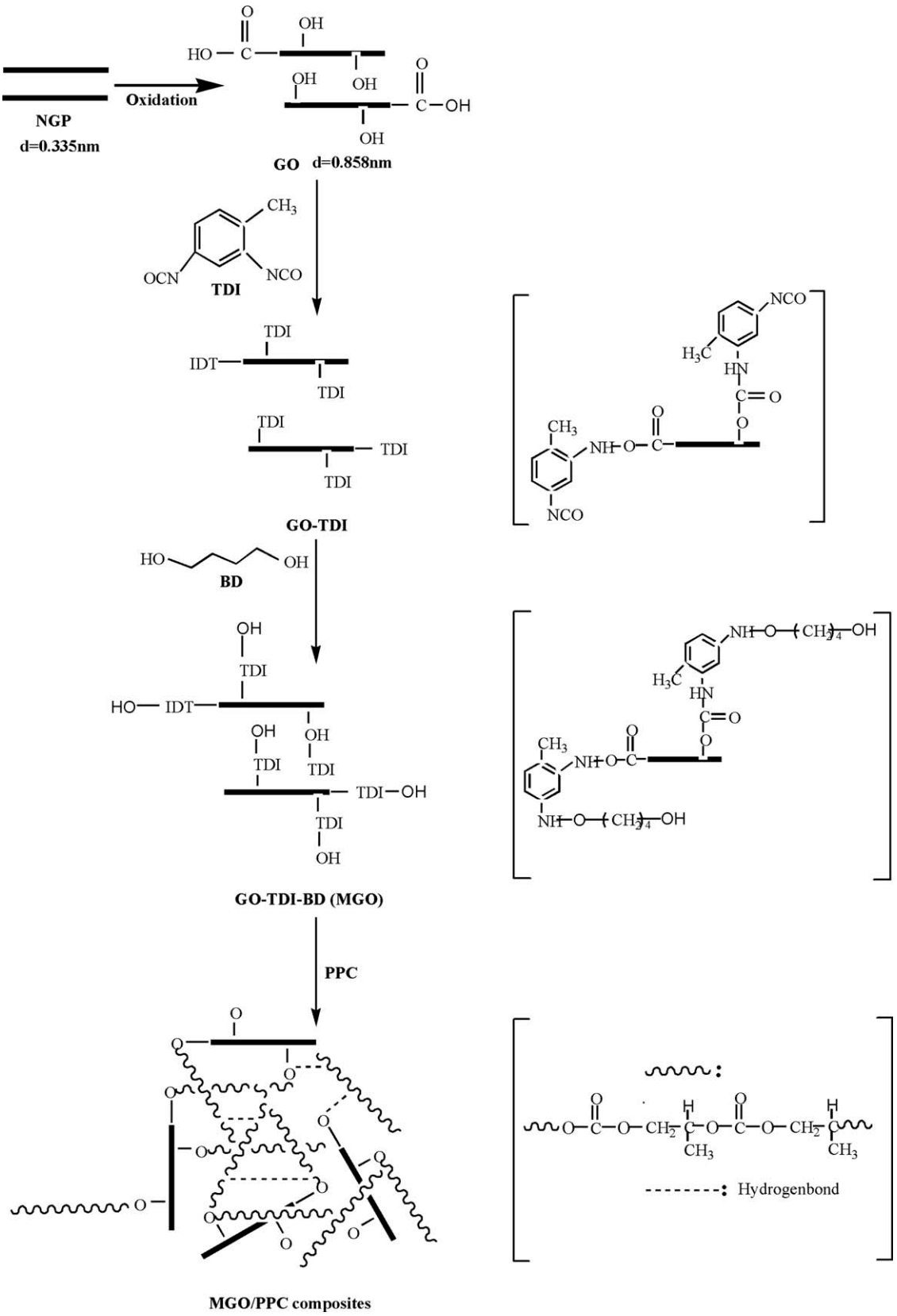

Scheme 1 Synthetic route of MGO/PPC composites.

rapidly remove any remaining solvent. After the solvent was completely removed, the composite film was taken out and dried for further analyses.

Characterization

Microscopy and structure

The morphology of samples were studied by SEM (JEOL JSM-820). The samples were gold coated before SEM examination. AFM image was taken on a SPM-9600 scanning probe microscope (Shimadzu). All images were collected under ambient conditions at 50% relative humidity and 23°C with a scanning raster rate of 1 Hz.

X-ray diffraction

The test was performed on a Rigaku D/max-1200X Diffractometer (Cu $K\alpha$ radiation ($\lambda = 0.154$ nm)) at ambient temperature. Scans were taken from 1.5° to 40° with a step of 0.02° at 40 kV and 30 mA. The NGP, GO, and GO-TDI-OH samples were in fine powder form, while GO/PPC composites samples were compressed thin slices.

Fourier transform infrared spectroscopy

The FTIR spectrum was observed at room temperature on a Nicolet 380 spectrometer (Thermo Electron Corp., Massachusetts, USA) with a resolution of 4 cm^{-1}. The specimens were dispersed into the KBr powder by mortar, and compressed to form disks.

Thermogravimetric analysis

The thermal stability of materials was measured by thermogravimetric analysis (TGA) on a Perkin–Elmer TGA-7 instrument. The samples were gradually heated at a rate of 20 °C/min from 30 to 500°C under N_2 gas flow rate of 20 mL/min. The weight loss/temperature curves were monitored.

Differential scanning calorimetric analysis

The thermal properties and glass transition temperature (T_g) of composites were analyzed by a NETZSCH DSC 200 F3 differential scanning calorimeter thermal analyzer in a N_2 environment. The samples were heated at a rate of 20 °C/min from −30 to 70°C, then quenched to −30°C and finally heated again to 70°C at a rate of 20 °C/min. The T_g was obtained from the second heating run.

Dynamic mechanical analysis

The DMA test was carried out on a TA Instruments DMA 2980 system in film tension mode at a fixed frequency of 1 Hz. The samples were cut from the compressed sheet, with dimensions $30 \times 6 \times 1$ mm^3. The measurement temperature range was from −100 to 40°C at atmospheric pressure. The other parameters are: heating rate was 5 °C/min; preload was 1 N, and the amplitude was 7.5 μm.

Tensile test

Tensile properties were tested on an INSTRON3365 electronic tensile tester with a computer controlling system. The testing specimen with a dimension of $5 \times 70 \times 0.1$ mm^3 was cut from the films of PPC and composites. The rate of cross-head motion was 10 mm/min at 20°C. Five specimens of each composition were tested, and the average values were reported.

RESULTS AND DISCUSSION

Structure and morphology of MGO and MGO/PPC composites

According to the Scheme 1, it was found that graphite derivative was prepared firstly using a modifier TDI with bi-functional groups. The amide and carbamate esters were formed by treatment of GO with TDI, which lead to the derivatization of both the edge of carboxyl and surface hydroxyl functional groups. Then, the GO-TDI was modified by BD to afford the hydroxyl functional groups on the surface of GO through the "grafting to" method. Then, MGO/PPC composites were formed with various amounts of layered GO-TDI-BD. Figure 1a shows the FTIR spectra of NGP, GO, and MGO (GO-TDI-BD). NGP surface shows inert character and no peak can be found in the spectra. GO shows four sharp peaks, 3431, 1729, 1631, and 1050 cm^{-1}, corresponding to the -OH, C=O, free water, and C—O—C group, respectively.[32] Upon treatment with TDI and BD, the C=O stretching vibration at 1729 cm^{-1} of GO becomes obscured by the appearance of a absorption peak at 1700 cm^{-1} that is attributable to the carbonyl stretching vibration of the carbamate esters of the GO-TDI-BD. A band at 1650 cm^{-1} could be assigned to the amide carbonyl stretching mode. The band at 1540 cm^{-1} is originated from either amides or carbamates esters and corresponds to the coupling of the C—N stretching vibration with the CHN deformation vibration.[30] The 1220 cm^{-1} band corresponds to the C—OH stretching vibration.

The interaction of polymer composites could be identified by FTIR spectra. It was known that, if two polymers were compatible, a distinct interaction (hydrogen-bonding or dipolar interaction) existed between the chains of one polymer and those of the other, causing the infrared spectra of the composites

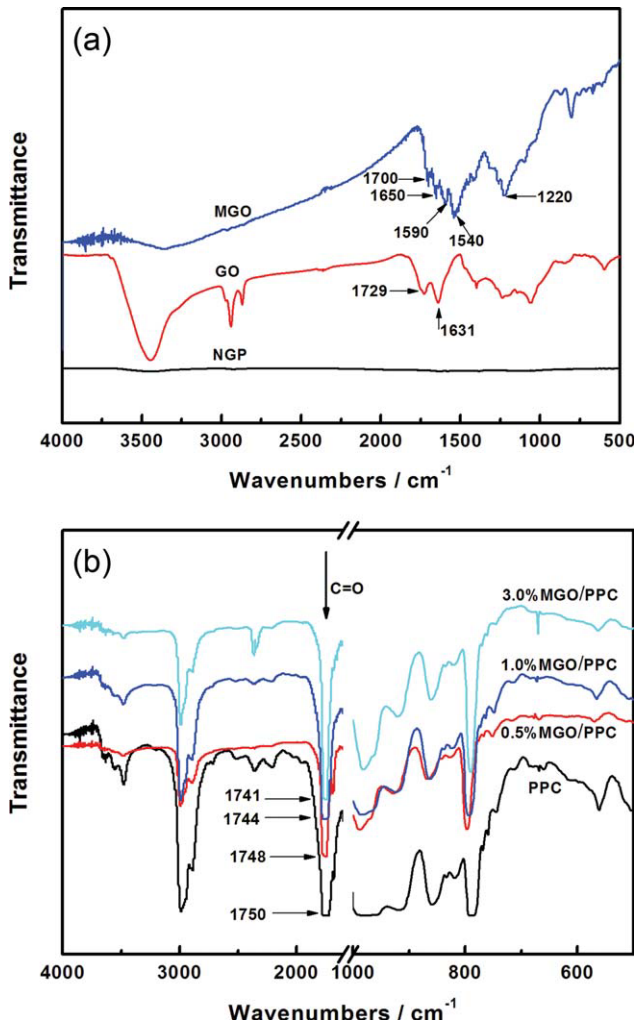

Figure 1 FTIR spectra of (a) NGP, GO, and MGO and (b) MGO/PPC composites with different MGO contents (The numbers *X* in PPC/*X* % MGO refer to the weight percent of MGO in composites). [Color figure can be viewed in the online issue, which is available at wileyonlinelibrary.com.]

to change (e.g., band shifts, broadening).[33] On the basis of the harmonic oscillator model, the reduction in force constant f can be represented by[34]:

$$\Delta f = f_b - f_{\mathrm{nb}} = \frac{\mu(\nu_b^2 - \nu_{\mathrm{nb}}^2)}{4\pi^2} \quad (1)$$

where $\mu = m_1 m_2/(m_1 + m_2)$ corresponded to the reduced mass of the oscillator, ν the oscillating frequency and f the force constant. The subscripts b and nb denote bonded and nonbonded oscillators, respectively. The reduction of force constant brought about by some interaction is directly related to the frequency (or wavenumber) shift of stretching vibrations. Thus, the lower the wavenumber corresponding to absorption peak, the stronger is the hydrogen bond interaction between polymer composites. In this sense, FTIR could identify segment interactions and obtain information about the phase behavior of polymer composites. Figure 1(b) shows the spectra of PPC and MGO/PPC composites with different MGO contents at room temperature in the carbonyl stretching region. PPC had a strong carbonyl stretching absorption at about 1750 cm^{-1}. With the increase of MGO content in MGO/PPC composites, the absorption peak shifts towards lower wavenumber. For 0.5 wt % MGO/PPC composite, the wavenumber corresponding to absorption peak is 1748 cm^{-1}, about 2 cm^{-1} lower than that for pure PPC. For 1.0 wt % MGO/PPC composite, the wavenumber corresponding to absorption peak is 1744 cm^{-1}, about 6 cm^{-1} lower than that for pure PPC. Because MGO is multi-hydroxyl filler, the shift of carbonyl stretching absorption to lower wavenumber is ascribed to the interaction between carbonyl groups of PPC and hydroxyl groups of MGO by hydrogen bonding. With the further addition of MGO, the C=O peak of PPC at 1750 cm^{-1} shifted to a lower wave number by 9 $cm^{-1}$when the MGO content increased from 0 to 3.0 wt %. Obviously, modification of GO can improve the interaction between PPC and graphite, indicating that the proposed route works.

There are two complimentary techniques to characterize the structure of composites: XRD and SEM, where the former reveals the change of *d*-spacing of graphite gallery while the later shows the morphological structure of composites. Figure 2 shows the XRD patterns of NGP, GO, GO-TDI, GO-TDI-BD, 0.5 wt % MGO/PPC, 1.0 wt % MGO/PPC, and 3.0 wt % MGO/PPC samples. According to Figure 2, the original NGP shows a (002) diffraction peak at $2\theta = 26.6°$, which corresponds to the *d*-spacing of 0.335 nm (curve a). Upon oxidation and modification, a weak

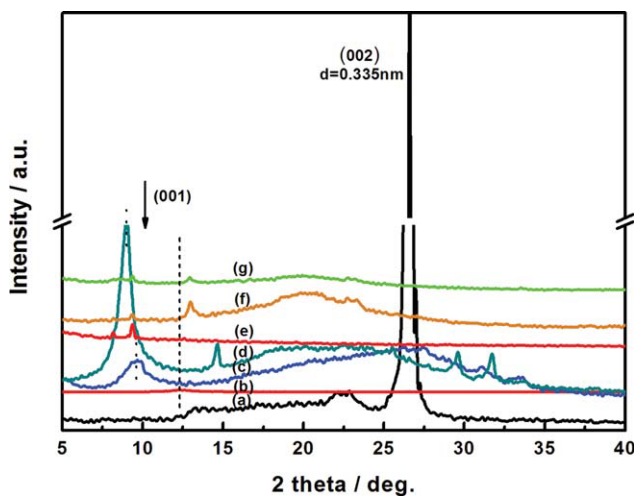

Figure 2 XRD patterns of samples. Curves from (a) to (g) denotes NGP, GO, GO-TDI, MGO, and MGO/PPC composites with 0.5, 1.0, and 3.0 wt % MGO contents. [Color figure can be viewed in the online issue, which is available at wileyonlinelibrary.com.]

diffraction peak of GO is observed at about $2\theta = 12.1^\circ$, (001) corresponding to the interlayer spacing of 0.858 nm (curve b), while that of the GO-TDI-BD platelets shifts to low $2\theta = 8.8^\circ$ and thus the interlayer spacing is increased to 1.3 nm due to the presence of the TDI and BD between the sheets of the GO (curve d). After organic modification, it was found that the organic modified MGO could not disperse well in water and finally precipitated. This phenomenon reveals that the surface of graphene platelets changed from hydrophilic one into hydrophobic one and this change is favorable for the interaction of organic polymer chains. Meanwhile, curves from e to g show the XRD patterns of MGO/PPC with different MGO contents. It was found that the initial diffraction peak (001) of MGO shifted from $2\theta = 8.8^\circ$ to a lower degree of diffraction angle ($2\theta = 8.1^\circ$) after blending with PPC. This result is ascribed to the intercalation of PPC macromolecular chains into hydrophobic graphene layers, resulting in the enlargement of interlayer distance of MGO. The (001, $d = 1.5$ nm) diffraction peak of MGO/PPC composites with MGO contents of 0.5 wt % located at $2\theta = 8.1^\circ$, which indicates that the intercalation of PPC chains increases the d_{001} spacing of NGP for about 1.2 nm. In the case of PPC/1.0 wt % MGO and 3.0 wt % MGO/PPC composites, there are small peaks appearing at $2\theta = 7.9^\circ$ corresponding to a d-spacing of 1.7 nm, which indicates that the intercalation of PPC chains increases the d_{001} spacing of NGP for about 1.4 nm.

The morphological structure of polymer composites is a very important characteristic because it ultimately determines many properties of the polymer composites, such as thermal stability and mechanical properties. In the present study, PPC is an aliphatic polycarbonate, which is hydrophobic. GO is a filler with multi-functional groups, which is hydrophilic. Obviously, GO/PPC composites will show very limited compatibility if they are simply blended. Now, GO was firstly treated with TDI to create the anchor sites on GO. Then, GO-TDI was reacted with BD through the "grafting to" method to afford hydroxyl groups on the surface of GO. The BD-derived hydroxyl groups on the surface of GO will be effective as "grafting points" of PPC and effectively improves the interfacial adhesion between PPC and graphite, and the improved interfacial adhesion results in increased compatibility. As shown in Scheme 1, the improved interfacial adhesion attributes to the strong chemical and physical interaction. Figure 3 shows the typical morphological structure of MGO/PPC composites. The as-received NGP shows the expected layered structure with relatively small interlayer's spacing [Fig. 3(a)]. However, the layer distance enlarged and the boundary layer was crimped after oxidative treatment [Fig. 3(b)]. The obtained GO shows strongly hydrophilic, and a mild ultrasonic treatment of GO in water results in its exfoliation to form stable aqueous dispersions that consist almost entirely of 1 nm thick sheets, as determined by AFM [Fig. 3(c) and the insert]. As illustrated in the Experimental section, to make GO dispersion within a polymer matrix at the individual sheet level possible, MGO was prepared by treating GO with organic isocyanates (TDI). The isocyanate treatment reduces the hydrophilic character of graphene oxide sheets by forming amide and carbamate ester bonds to the carboxyl and hydroxyl groups of GO, respectively. As a result, such isocyanate-derivatized GOs no longer exfoliate in water but readily form stable dispersions in polar aprotic solvents (such as DMF), as shown in [Fig. 3(e)]. Also, these dispersions of isocyanate-derivatized GOs allow graphene oxide sheets to be intimately mixed with many organic polymers, facilitating the synthesis of graphene–PPC composites [Fig. 3(f–i)]. Figure 3(j,k) show the SEM images of MGO/PPC composites. It clearly shows that MGO has been well dispersed throughout the PPC matrix [Fig. 3(j,k)]. As we all known that the quality of nanofiller dispersion in the polymer matrix directly correlates with its effectiveness for improving mechanical, thermal, impermeability, and other properties. The properties of a composite are also intimately linked to the aspect ratio and surface-to-volume ratio of the filler. The potential properties of our graphene sheet-based composites thus appear promising owing to the extremely high aspect ratios of the sheets as determined from SEM images [Fig. 3(j,k)], in which the average lateral dimension was estimated to be ~ 1 μm, similar to the values found by AFM [Fig. 3(c)]. The fine dispersion of graphene sheets may contribute to the properties increment, which will be further confirmed in the next section.

TGA results of MGO/PPC composites

It has been known that the poor thermal stability and low glass transition temperature (T_g) of PPC have limited its application. Many efforts have been devoted to improve the thermal property of PPC. An effective method is to modify the PPC chain structure by adding maleic anhydride to the end of PPC molecular chain. In the case of graphite intercalated composites, the graphite layers can retard the thermal degradation of polymer due to its good thermal insulation effect. Furthermore, the graphite intercalated composites could be prepared more simply and conventionally compared to the chemical modification of PPC chains. Considering above-mentioned, TGA is performed for the composites to prove the improvement of the thermal property of PPC when MGO is incorporated, where the weight loss due to the volatilization of the degradation products is monitored as a function of temperature.

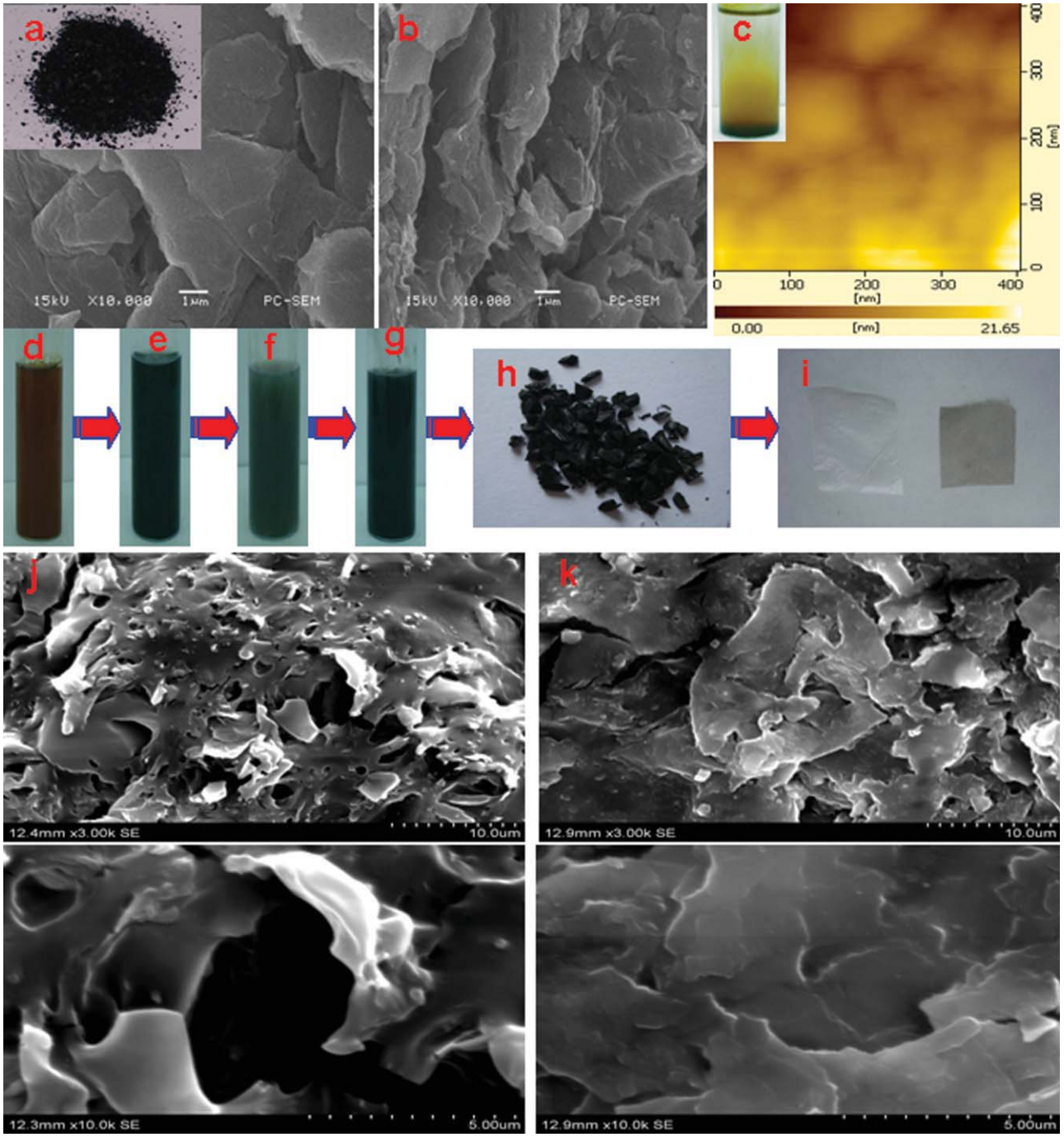

Figure 3 Images of samples after receiving different treatments. (a) SEM and digital image (inset) of NGP. (b) SEM image of GO. (c) A typical AFM noncontact-mode image of GO sheets deposited onto a mica substrate from an aqueous dispersion (inset). (d, e) Suspension of GO (d) and phenyl isocyanate-treated GO (1 mg ml^{-1}) in DMF (e). (f, g) Suspension of 0.5 wt % MGO/PPC/ (f) and 3.0 wt % MGO/PPC composites in DMF. (h) Composite powder as obtained after coagulation in methanol. (i) The films of pure PPC (left) and 3.0 wt % MGO/PPC composites (right). (j, k) Low (top row) and high (bottom row) magnification SEM images obtained from a fracture surface of composite samples of: (j) 1.0 wt % (left) and (k) 3.0 wt % (right) MGO in PPC. [Color figure can be viewed in the online issue, which is available at wileyonlinelibrary.com.]

Figure 4 shows the TGA and differential thermal analysis (DTG) of MGO/PPC composites with different MGO contents. Compared with pure PPC, the thermal stability of MGO/PPC composites is improved due to the shielding effect of MGO layers, as shown in Figure 4(a). The TGA analysis data is summarized in Table I. Here, the $T_{0.05}$ represents the onset temperature of thermal degradation when 5% weight lost, while $T_{0.5}$ is the temperature regarded as the midpoint of the degradation process when

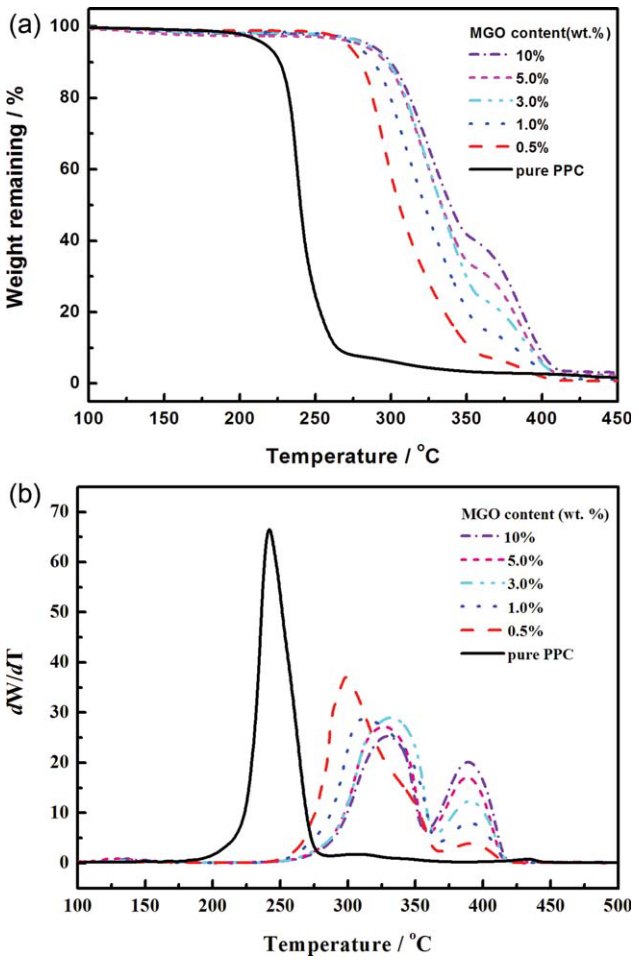

Figure 4 TGA analysis of PPC and MGO/PPC composites with different MGO contents: (a) weight loss curves, (b) derivative of the weight loss curves shown in (a). [Color figure can be viewed in the online issue, which is available at wileyonlinelibrary.com.]

50% degradation occurred. As shown in Table I, all the MGO/PPC composites show an obviously higher thermal stability than pure PPC, and the thermal stability of MGO/PPC increases with increasing MGO contents. This indicates the positive effect of MGO on the thermal stability of the composites. However, the thermal stability of composites levels off after MGO content increases to 5.0 wt %. It was reported that the thermal decomposition behavior of a polymer is influenced by many factors, such as heating rate, surrounding atmosphere, sample weight, and shape.[35] From the DTG results in Figure 4(b), it can be seen that the fastest thermal decomposition temperatures are improved after the addition of MGO, and about 90°C higher than that of PPC. The curves of composites become wider than that of pure PPC. The incorporation of MGO into the PPC matrix would enhance its thermal stability by acting as a superior insulator. The graphite layers which uniformly disperse in matrix lead to the difficulty in heat conduction and acts as a mass transport barrier to the volatile products which generate during decomposition. Those functions of graphite layers will result in the lag and wide peaks of composites during decomposition. In addition to the observation of the fastest thermal decomposition rate in range of 290–330°C for all MGO/PPC composites, a small peak around 400°C was found for all MGO/PPC composites. This maybe ascribed to the uneven dispersion of MGO when the MGO content is too high.

TABLE I
Thermal Properties of Pure PPC and MGO/PPC Composites

MGO (wt %)	0	0.5	1.0	3.0	5.0	10
$T_{0.05}$ (°C)	218	271	277	283	286	290
$T_{0.5}$ (°C)	240	305	322	334	338	340
T_g[a] (°C)	28.1	32.4	36.3	41.9	41.6	–
T_g[b] (°C)	30.6	32.7	38.1	41.7	42.2	–

[a] Obtained from DSC analysis.
[b] Obtained from DMA analysis. "–": cannot be detected.

DSC and DMA results of MGO/PPC composites

The DSC traces of both PPC and MGO/PPC composites are shown in Figure 5. The pure PPC exhibits a glass transition temperature (T_g) at 28.1°C. With the addition of MGO, the T_g values of MGO/PPC composites obviously increase, and the composites with MGO content 3.0 wt % shows the highest T_g at 41.9°C, which is 13.8°C higher than that of PPC. This is because of the strong interaction between the polymer and the nano-dispersed graphite layers, which restricts the segmental motion of PPC molecular chains. The improvement of both the decomposition temperature and glass transition temperature of composites indicates that composition is an efficient way to increase the thermal stability of PPC.

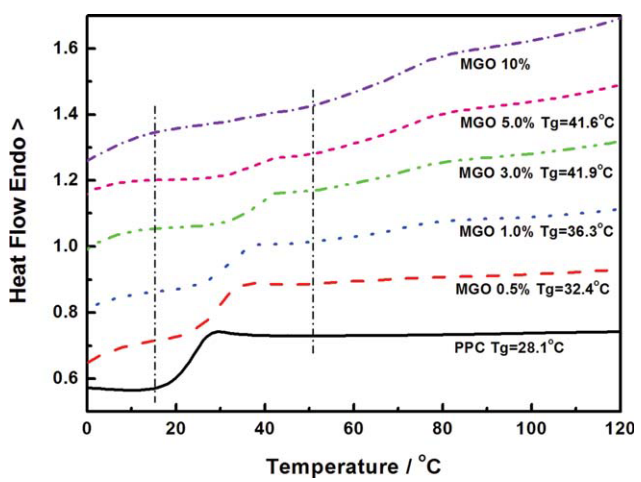

Figure 5 DSC curves of PPC and MGO/PPC composites with different MGO contents. [Color figure can be viewed in the online issue, which is available at wileyonlinelibrary.com.]

DMA is one of the techniques commonly used to characterize the time, frequency, and temperature dependency of the viscoelastic nature of polymers. It have been reported in the literature[33,34] that the addition of graphite could increase both the storage modulus (E) and T_g for composites. The DMA results obtained from the current study is shown in Figure 6(a), which agrees with the reported literatures. In particular, the E is greatly improved with the increase of MGO content. For example, the composite with 3.0 wt % of MGO exhibits a very high E value of 16,683 MPa at 30°C, which is two times more than that of pure PPC (about 6905 MPa). The significant improvement in E value of MGO/PPC composites is ascribed to the combined effect of high performance and fine dispersion of high aspect ratio MGO filler. The T_g, which represents one of the major viscoelastic transitions of a material, is often obtained from the maximum of the tangent delta (tan δ) curve as shown in Figure 6(b). The results show that the T_g shifts to higher temperature as MGO content increases, and the T_g for the composite that contains 3.0 wt % of MGO has been raised by nearly 8°C when compared with of pure PPC. The increase in T_g is related to the confinement effect from MGO platelets, thus usually increasing the T_g of the composites. The T_g data obtained from DMA analysis are slightly different from data from DSC characterization (Table I). This is resulted from different test methods used.

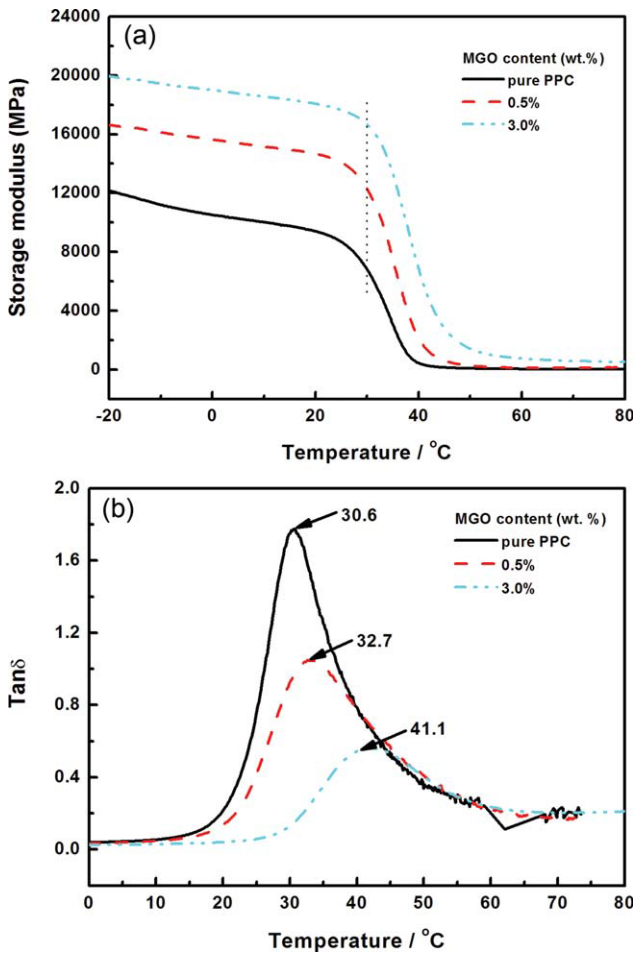

Figure 6 DMA measurements of MGO/PPC composites: (a) storage modulus; and (b) tangent delta. [Color figure can be viewed in the online issue, which is available at wileyonlinelibrary.com.]

Tensile properties of the MGO/PPC composites

Interfacial interaction between the fillers and matrix is an important factor affecting the mechanical properties of the resultant composites. Strong interfacial interaction is favorable to enhance the mechanical properties because weak interfacial interaction will result in weak interfacial layer, which cannot transfer stress effectively. In this work, the tensile strength and Young's modulus as representative mechanical properties were measured for the MGO/PPC composites with MGO contents from 0 to 10.0 wt %. Figure 7 shows the mechanical properties of composites as a function of MGO contents. For comparative purposes, the tensile values of NGP/PPC (NGP content: 3.0 wt %) and GO/PPC (GO content: 3.0 wt %) composites are also shown. It was found that both the tensile strength and Young's modulus of composites increased with MGO addition. When the MGO content is 3.0 wt %, the composite shows the highest tensile strength as 29.5 MPa which is two times higher than that of pure PPC. At the same time, it shows the highest Young's modulus as 1.93 GPa, while the Young's modulus of PPC is only 0.87 GPa. Further addition of MGO such as the composites with 5.0 wt % MGO leads to the decrease of mechanical properties. Nevertheless, all MGO/PPC composites show improved mechanical properties than pure PPC in our experimental conditions. The improvement of mechanical properties can be attributed to two reasons.

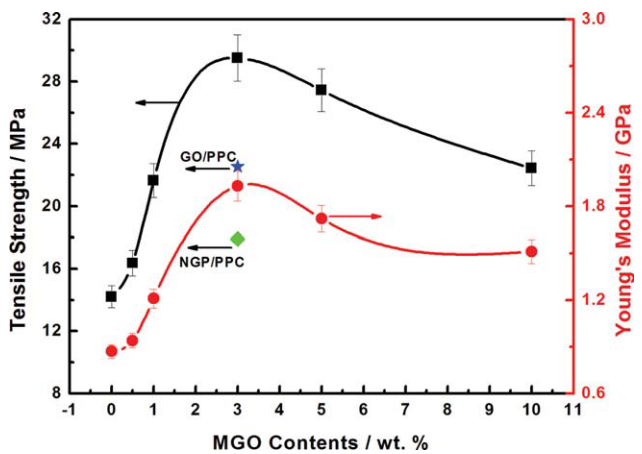

Figure 7 Mechanical properties of PPC, GO/PP, NGP/PPC, and MGO/PPC composites with different MGO contents. [Color figure can be viewed in the online issue, which is available at wileyonlinelibrary.com.]

The first reason is explained as the disordered MGO platelets dispersed finely in the PPC matrix, the other reason is due to the PPC chain grafting on the surface of MGO which increases the interaction between PPC chain and MGO. As confirmed by the IR and TG results, the organic-modified GO have strong interfacial interaction with the PPC matrix. These strong interaction and the excellent properties of MGO lead to the significant increase in both thermal and mechanical properties of the composites. However, as the MGO content continuously increases, some graphite layers begin to aggregate. The formation of large graphite aggregates will effectively reduce the interfacial area between polymer and graphite layers. Furthermore, these aggregates will act as stress concentrators to diminish the mechanical properties of the composites.

CONCLUSIONS

This work was devoted to prepare a novel MGO/PPC composite by solution intercalation method and to study the effects of MGO incorporation on the properties (especially thermal and mechanical properties) of PPC. The results achieved can be summarized as follows:

1. FTIR analysis showed that TDI and BD have been "grafted" on the layers of graphite. The dispersibility of GO in the organic media was improved after modification by using TDI and BD. And the modified GO afforded active hydroxyl groups on the surface of MGO, which provided an effective way to form MGO/PPC composites in solution phase. The functionalization of GO played an important role in the fabrication of MGO/PPC composites.
2. XRD analysis revealed that PPC chains have been intercalated into the layers of MGO, resulting in the increase of layer distance. SEM images showed that the composites have a uniform structure. Graphite showed a well dispersion in the PPC matrix.
3. TGA, DSC, and DMA results showed that the thermal stability and glass transition temperature of PPC are improved by adding MGO into PPC matrix. The MGO/PPC composites with 3.0 wt % MGO shows the highest thermal stability and the T_g is 13.8°C higher than that of pure PPC.
4. Tensile tests showed that when the MGO content is 3.0 wt %, the composite has the highest tensile strength as 29.51 MPa, which is about two times higher than that of pure PPC.
5. Those improvements could be attributed to the improved interfacial compatibility between PPC matrix and good dispersion of MGO in PPC matrix. In conclusion, the composition provides an efficient way to prepare biodegradable inorganic filler–PPC composites, to improve both the thermal and mechanical properties of PPC and consequently widely expands its application fields in the future.

The authors thank Dr. F. G. Du (TianGuan Group, Hei-Nan, China) for providing the PPC samples. AFM and DMA tests from Sichuan University are gratefully acknowledged.

References

1. Inoue, Y.; Yoshie, N. Prog Polym Sci 1992, 17, 571.
2. Okada, M. Prog Polym Sci 2002, 27, 87.
3. Peng, S. W.; An, Y. X.; Chen, C.; Fei, B.; Zhuang, Y. G.; Dong, L. S. Polym Degrad Stab 2003, 80, 141.
4. Lai, M. F.; Li, J.; Liu, J. J. T. J Therm Anal Calorim 2005, 82, 293.
5. Li, X. H.; Meng, Y. Z.; Wang, S. J.; Rajulu, A. V.; Tjong, S. C. J Polym Sci, Part B: Polym Phys 2004, 42, 666.
6. Ge, X. C.; Li, X. H.; Zhu, Q.; Li, L.; Meng, Y. Z. Polym Eng Sci 2004, 44, 2134.
7. Li, X. H.; Tjong, S. C.; Meng, Y. Z.; Zhu, Q. J Polym Sci Part B: Polym Phys 2003, 41, 1806.
8. Tsuji, H.; Kawashima, Y.; Takikawa, H.; Tanaka, S. Polymer 2007, 48, 4213.
9. Chung, D. D. L. J Mater Sci 2002, 37, 1475.
10. Zhang, M.; Li, D.; Wu, D.; Yan, C.; Lu, P.; Qiu, G. J Appl Polym Sci 2008, 108, 1482.
11. Zheng, W.; Wong, S.; Sue, H. Polymer 2002, 43, 6767.
12. Hua, L.; Kai, W.; Inoue, Y. J Appl Polym Sci 2007, 106, 1880.
13. Kai, W. H.; Hirota, Y.; Hua, L.; Inoue, Y. J Appl Polym Sci 2007, 107, 1395.
14. Xu, J.; Li, R. K.; Meng, Y. Z.; Mai, Y. W. Mater Res Bull 2006, 41, 244.
15. Xu, J.; Li, R. K.; Xu, Y.; Li, L.; Meng, Y. Z. Eur Polym Mater 2005, 41, 881.
16. Du, L. C.; Qu, B. J.; Meng, Y. Z.; Zhu, Q. Compos Sci Technol 2006, 66, 913.
17. Zhang, Z. H.; Shi, Q.; Peng, J.; Song, J. B.; Chen, Q. Y.; Yang, J. L. Polymer 2006, 47, 8548.
18. Cui, L.; Tarrte, N. H.; Woo, S. I. Macromolecules 2008, 41, 4268.
19. Zhao, Q.; Samulki, E. T. Macromolecules 2005, 38, 7967.
20. Shah, R. K.; Paul, D. R. Polymer 2006, 47, 4075.
21. Huang, Y. J.; Yang, K. F.; Dong, J. Y. Macromol Rapid Commun 2006, 27, 1278.
22. Han, Y.; Lu, Y. Carbon 2007, 45, 2394.
23. Matsuo, Y.; Miyabe, T.; Fukutuka, T.; Sugie, Y. Carbon 2007, 45, 1005.
24. Wang, G.; Yang, Z.; Li, X.; Li, C. Carbon 2005, 43, 2564.
25. He, H.; Klinowski, J.; Forster, M.; Lerf, A. Chem Phys Lett 1998, 287, 53.
26. Hirata, M., Gotou, T.; Ohba, M. Carbon 2005, 43, 503.
27. Liu, P.; Gong, K.; Xiao, P.; Xiao, M. J Mater Chem 2000, 36, 933.
28. Stankovich, S.; Piner, R. D.; Nguyen, S. T.; Ruoff, R. S. Carbon 2006, 44, 3342.
29. Stankovich, S.; Dikin, D. A.; Dommett, G. H. B.; Kohlhaas, K. M.; Zimney, E. J.; Stach, E. A.; Piner, R. D.; Nguyen, S. T.; Ruoff, R. S. Nature 2006, 442, 282.
30. Xu, C.; Wu, X.; Zhu, J.; Wang, X. Carbon 2008, 46, 386.
31. Ranjan, R.; Brittain, W. Macromolecules 2007, 40, 6217.
32. Bian, J.; Xiao, M.; Wang, S. J.; Wang, X. J.; Lu, Y. X.; Meng, Y. Z. Chem Eng J 2009, 147, 287.
33. Peng, S. W.; Wang, X. Y.; Dong, L. S. S. Polym Compos 2005, 26, 37.
34. Pawlak, A.; Mucha, M. Thermochim Acta 2003, 396, 153.
35. Quan, H.; Zhang, B. Q.; Zhao, Q.; Yuen, R. K. K.; Li, R. K. Y. Compos A 2009, 40, 1506.